Preprints of the 21st IFAC World Congress (Virtual)
Berlin, Germany, July 12-17, 2020

Dynamic matrix control of thermal power for multiple nuclear steam supply system modules

Di Jiang, Zhe Dong

**Institute of Nuclear and New Energy Technology (INET), Collaborative Innovation Center of Advanced Nuclear Energy Technology of China, Key Laboratory of Advanced Reactor Engineering and Safety of Ministry of Education, Tsinghua University, Beijing 100084, China (e-mail: fyjiangdi@mail.tsinghua.edu.cn, dongzhe@mail.tsinghua.edu.cn)}*

Abstract: To suppress the fluctuation from both load side and intermittent renewable energy (IRE), nuclear power plants (NPPS) should be operated in load-following mode to improve economic competitiveness. The modular high temperature gas-cooled reactor (MHTGR) belongs to the category of small nuclear reactor and is suitable for load-following by the virtue of online refueling ability and inherent safety. To realize economies of scale for MHTGR, multi-modular scheme that multiple nuclear steam supply system (NSSS) modules are connected in parallel providing superheated steam for common turbine is recommended to achieve desired power ratings. However, because of the large heat capacity in the pebble-bed of MHTGR and thermal coupling of different NSSSs through common secondary loop fluid network, the current control strategy which suppresses the nuclear power, coolant temperatures measurement from their set-points without considering thermal dynamic of NSSS itself, may not favorable for heat transfer in the NSSS. To improve the load-following ability, a multivariable dynamic matrix control (DMC) is constituted to dynamic compensate the thermal energy variation of NSSS. The implementation of the DMC has a typical cascade structure, where DMC revises the set-points of NSSS module in outer loop and the existing PID control law is adopt for stabilization in inner loop. Numerical results show that this cascade dynamic matrix control can improve the transient of thermal power under power maneuvering.

Keywords: Multi-nuclear steam supply systems, cascade control, dynamic matrix control, thermal power optimization, modular high temperature gas-cooled reactor.

1. INTRODUCTION

Due to the deep penetration of intermittent renewable energy (IRE) such as solar and wind power, there has been intense competition among energy suppliers in the energy market. Therefore, with the increase of the capacity of nuclear power in China, the requirements for safe and economic operation of any nuclear power plants (NPPs) are getting higher and higher (Lund et al., 2015; Alizadeh et al., 2016). To achieve this goal, NPPs need to be operated in load-following mode to meet the various load demands, determined by power grid dispatching signal or manually set from operator (Wood et al., 2014). Usually, NPPs involves energy conversion among nuclear energy, thermal energy, and electric energy. The power balance between thermal energy, electric energy and load is of great significance to the efficient and safe operation of NPPs (Dong et al., 2019). Since turbo-generator system is a relatively fast energy conversion process, the key of load-following of NPPs is the thermal power tracking ability to balance the load, while maintaining coolant temperatures and nuclear power at desired values.

Nuclear steam supply system (NSSS), which mainly consists of one nuclear reactor and one steam generator producing superheated/saturated steam, is the central device for converting nuclear power to thermal power of any NPPs. Generally, small modular reactors have inherent safety characteristics such as passive residual heat removal, low power density in Reactor Pressure Vessel (RPV), and compact primary circuit design (Locatelli et al., 2015), which can prevent core melting, radioactive release and coolant loss accidents (LOCA) (Bae et al., 2001). Therefore, compared with large pressurized water reactor (PWR), small modular reactors is more suitable to operate under load-following mode. The modular high temperature gas-cooled reactor (MHTGR) belongs to the category of small modular reactors adopting helium as the coolant and graphite as both the moderator and core structural material (Lanning et al., 1989). A MHTGR-based NSSS, which is composed with a MHTGR and a once-through steam generator (OTSG) for producing superheated steam at 13.24 MPa and 571 ℃, can be considered as an flexible and affordable candidate for power generation, desalinated water, hydrogen production, process heat, and hybrid energy systems incorporated with IRE (Garcia et al., 2016). Despite the inherent safety of MHTGR, the rated thermal power of MHTGR is less than one tenth of that of commercial large PWR. To achieve economies of scale, a multi-module scheme, i.e. multiple MHTGR-based NSSS modules driving a single turbo-generator system, can realize any expected power rating with inherent safety (Dong et al., 2018). However, as the number of MHTGR-based

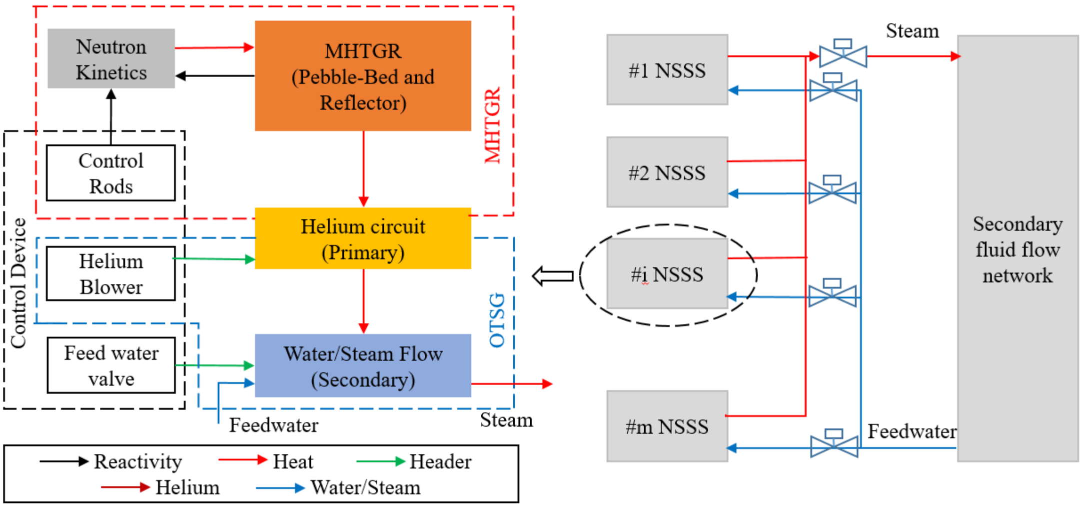

Fig. 1. The schematic diagram of the multiple MHTGR-based NPPs.

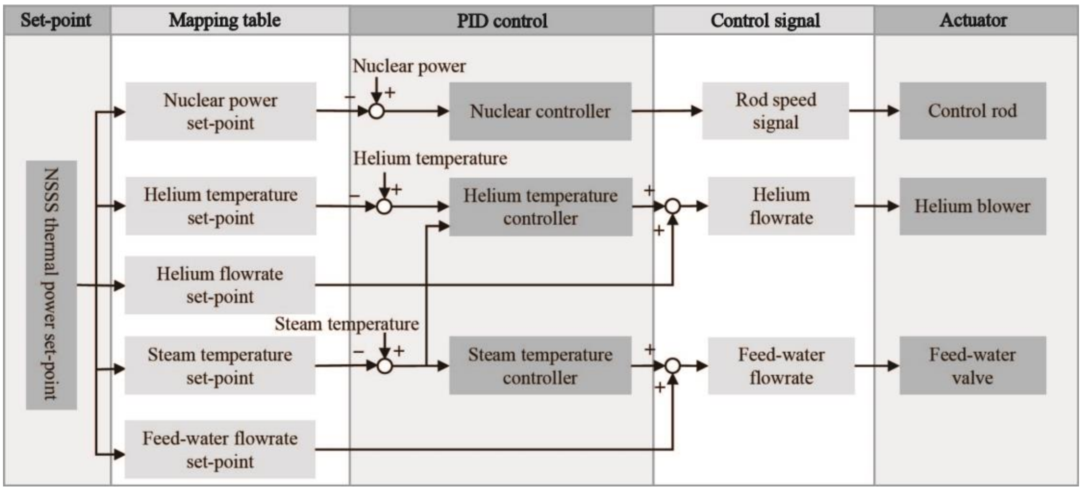

Fig. 2. Schematic diagram of a MHTGR-based NSSS coordinated PID control system.

NSSS modules increases, the power control of multi-modular high temperature gas-cooled reactor plants is quite different from those of single modular [Li et al., 2016]. The control inputs are computed to suppression the deviation of the measurements from their set-points, without compensation of thermal dynamic of NSSSs itself. Due to the thermal coupling among different NSSS and large specific heat capacity of MHTGR, the thermal power response may not be satisfactory, which is the major obstacles to suppress the fluctuation of both load side and IRE.

In this paper, based on the previous work [Jiang et al., 2018, 2019], DMC is utilized for the practical application of thermal power optimization for multi-modular high temperature gas-cooled reactor plants. DMC is a field-validated sampling-based algorithm, which is based on the so-called step response model (SRM) in many industrial practices (Moon et al., 2018). The data used to build SRM is easy to obtain, and the resultant online optimization problem is usually a quadratic programming (QP), which can be efficient solved by the state-of-art of convex optimization algorithm.

2. THERMAL POWER ANALYSIS OF MULTIPLE NSSS MODULES

2.1 Multi-modular NSSS

The schematic diagram of the multi-modular MHTGR is shown in Fig. 1, where several NSSS modules supply superheated steam to a common secondary fluid network. Each NSSS module includes the MHTGR, OTSG and control devices such as control rods, helium blower and feed-water valve. The nuclear fission power in pebble-bed is transferred to the secondary side of OTSG through helium circuit for power production. For stability of operation, a NSSS modular control scheme is shown in Fig. 2, which includes mapping tables, nuclear power controller, helium temperature controller and steam temperature controller (Dong et al., 2017). The NSSS set-point is given by power grid dispatching signal or manually set from operator. The mapping tables is a look-up table from thermal power set-point to set-points of flowrates, nuclear power and temperatures. Then these controllers, driven by the errors

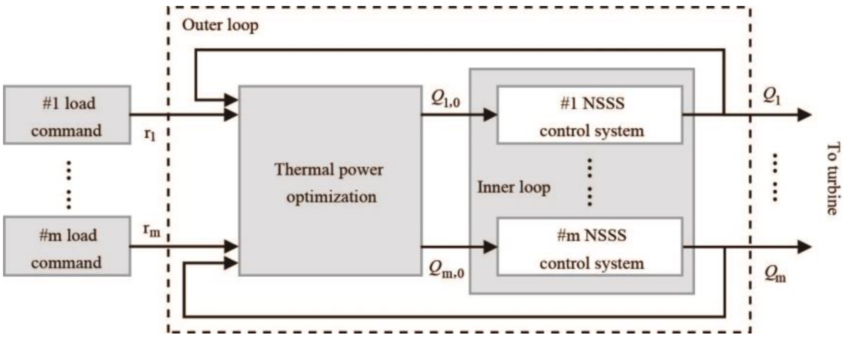

Fig. 3. Schematic diagram of cascaded control structure for multiple MHTGR-based NSSS.

between the set-points and corresponding measurements, output the control signals to adjust helium and feed-water flowrate through changing rotating speed of blower and opening of feed-water valve. Moreover, MHTGR-based NPPs is operated in turbine follow mode for reliability consideration. Accordingly, the steam valve is utilized to regulate the pressure, and the load following is achieved only by the NSSS control system.

2.2 Thermal power analysis

For thermal power analysis, assume that nuclear power has been well controlled by the rods, a simple temperature dynamic model of the i-th NSSS is (Dong et al., 2017):

$$\dot{E}_{\mathrm{i}} = A_{\mathrm{i}} E_{\mathrm{i}} + B_{\mathrm{i,s}} Q_{\mathrm{i},0} + B_{\mathrm{i,d}} T_{\mathrm{fw}} \tag{1}$$

where, $B_{\mathrm{i,d}} = \begin{bmatrix} 0 \\ 0 \\ 2M_{\mathrm{i,S}} \end{bmatrix}$, $B_{\mathrm{i,s}} = \begin{bmatrix} 1 \\ 0 \\ 0 \end{bmatrix}$, $E_{\mathrm{i}} := \begin{bmatrix} E_{\mathrm{i,R}} & E_{\mathrm{i,P}} & E_{\mathrm{i,S}} \end{bmatrix}^{\mathrm{T}}$,

$$A_{\mathrm{i}} = \begin{bmatrix} -\mu_{\mathrm{i,R}}^{-1}\Omega_{\mathrm{i,P}} & \mu_{\mathrm{i,R}}^{-1}\Omega_{\mathrm{i,P}} & 0 \\ \mu_{\mathrm{i,P}}^{-1}\Omega_{\mathrm{i,P}} & -\mu_{\mathrm{i,P}}^{-1}\left(\Omega_{\mathrm{i,P}} + \Omega_{\mathrm{i,S}}\right) & \mu_{\mathrm{i,P}}^{-1}\Omega_{\mathrm{i,S}} \\ 0 & \mu_{\mathrm{i,S}}^{-1}\Omega_{\mathrm{i,S}} & -\mu_{\mathrm{i,S}}^{-1}\left(\Omega_{\mathrm{i,S}} + 2M_{\mathrm{i,S}}\right) \end{bmatrix},$$

$\mathrm{i} = 1,2,\cdots,\mathrm{m}$, m is the number of i-th NSSS modules. $E_{\mathrm{i,R}}$, $E_{\mathrm{i,P}}$, $E_{\mathrm{i,S}}$ are the thermal energy stored in the pebble-bed, helium circuit and the secondary side of OTSG. $E_{\mathrm{i,R}} = \mu_{\mathrm{i,R}}^{-1} T_{\mathrm{i,R}}$, $E_{\mathrm{i,P}} = \mu_{\mathrm{i,P}}^{-1} T_{\mathrm{i,P}}$, $E_{\mathrm{i,S}} = \mu_{\mathrm{i,S}}^{-1} T_{\mathrm{i,S}}$. $T_{\mathrm{i,R}}$, $T_{\mathrm{i,P}}$, $T_{\mathrm{i,S}}$, T_{fw} are average temperatures of the pebble-bed, helium, OTSG secondary steam and feedwater, respectively. $\mu_{\mathrm{i,R}}$, $\mu_{\mathrm{i,P}}$, $\mu_{\mathrm{i,S}}$ are total heat capacity of the pebble-bed, the primary helium flow and the secondary water/steam flow, respectively. $\Omega_{\mathrm{i,P}}$ is heat transfer coefficient between the primary helium flow and MHTGR. $\Omega_{\mathrm{i,S}}$ is heat transfer coefficient between OTSG two sides and is positive correlation with helium flowrate. $M_{\mathrm{i,S}}$ is mass flowrate times its specific heat capacity of OTSG secondary flow. $Q_{\mathrm{i},0}$ is the i-th NSSS thermal power set-point. The equilibrium of (1) is,

$$\begin{cases} E_{\mathrm{i,R}} = \mu_{\mathrm{i,R}} T_{\mathrm{fw}} + \mu_{\mathrm{i,R}} Q_{\mathrm{i},0}\left[\dfrac{1}{\Omega_{\mathrm{i,P}}} + \dfrac{1}{\Omega_{\mathrm{i,S}}} + \dfrac{1}{2M_{\mathrm{i,S}}}\right] \\ E_{\mathrm{i,P}} = \mu_{\mathrm{i,P}} T_{\mathrm{fw}} + \mu_{\mathrm{i,P}} Q_{\mathrm{i},0}\left[\dfrac{1}{\Omega_{\mathrm{i,S}}} + \dfrac{1}{2M_{\mathrm{i,S}}}\right] \\ E_{\mathrm{i,S}} = \mu_{\mathrm{i,S}} T_{\mathrm{fw}} + \mu_{\mathrm{i,S}} Q_{\mathrm{i},0}\dfrac{1}{2M_{\mathrm{i,S}}} \\ \Omega_{\mathrm{i,S}} = \dfrac{Q_{\mathrm{i},0}}{T_{\mathrm{i,P}} - T_{\mathrm{i,S}}},\ M_{\mathrm{i,S}} = \dfrac{Q_{\mathrm{i},0}}{2\left(T_{\mathrm{i,S}} - T_{\mathrm{fw}}\right)} \end{cases} \tag{2}$$

And multipliy $e = \begin{bmatrix} 1 & 1 & 1 \end{bmatrix}^{\mathrm{T}}$ on both sides of equation (1), the total thermal power dynamic can be obtained as,

$$\begin{cases} \dot{E}_{\mathrm{i,t}} + Q_{\mathrm{i}} = Q_{\mathrm{i},0}, \quad \mathrm{i}=1,2,\cdots,\mathrm{m} \\ Q_{\mathrm{i}} = 2M_{\mathrm{i,S}}\left(T_{\mathrm{i,S}} - T_{\mathrm{fw}}\right) \end{cases} \tag{3}$$

where, Q_{i} is thermal power of i-th NSSS module, and $\dot{E}_{\mathrm{i,t}} = e^{\mathrm{T}}\dot{E}_{\mathrm{i}}$.

Because the heat capacity of pebble-bed with a large amount of graphite is significantly larger than that of OTSG filled with steam/water fluid, from (2), the thermal storage is mainly in the pebble-bed due to the large value of $\mu_{\mathrm{i,R}}$ and can be effectively extracted by adjusting $\Omega_{\mathrm{i,S}}$ and $M_{\mathrm{i,S}}$, which is realized by adjusting the helium and feed-water flowrate. Suppression of the temperature's deviation from their set-points would force the feedwater flowrate convergence to the value in (2) and hence may not favourable for heat exchange. Equation (3) shows that Q_{i} results from $Q_{\mathrm{i},0}$ and is disturbed by $\dot{E}_{\mathrm{i,t}}$. For the control scheme in Fig. 2, the thermal power command is directly fed to the NSSS module control system without further consideration the dynamic of NSSS. Thus Q_{i} would inherit the slow dynamic of NSSS due to the large heat capacity in the pebble-bed. Moreover, due to the feed-water preheating system in the secondary fluid network, T_{fw} is positively correlated with the nuclear island thermal power. The variation of T_{fw} caused by power manoeuvre of any NSSS module will influence thermal power of other module through the common feed-water temperature. From the above analysis, although the global stability can be guaranteed by the control scheme, thermal power response may be unsatisfactory. Since the thermal power cannot be

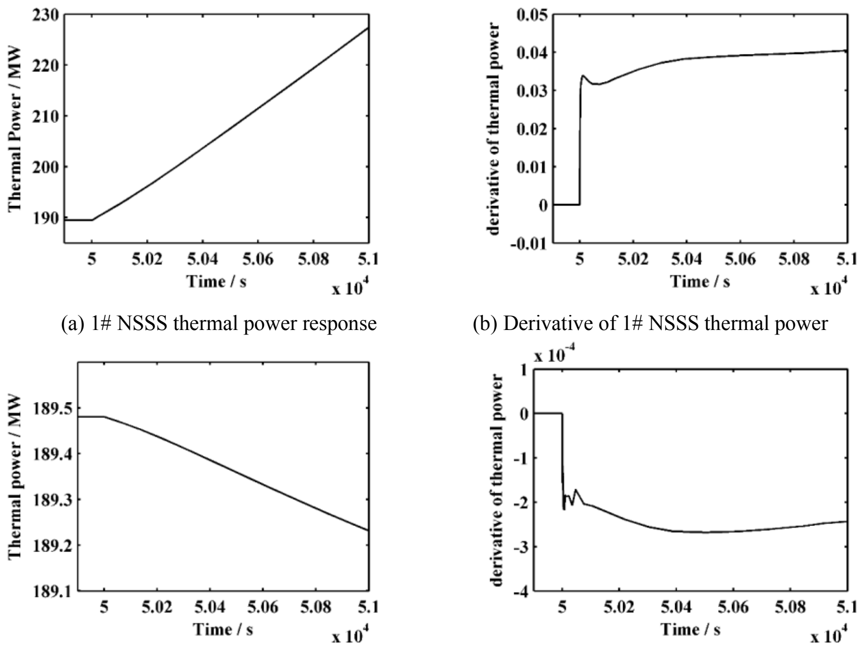

(a) 1# NSSS thermal power response

(b) Derivative of 1# NSSS thermal power

c) Other NSSS thermal power response

(d) Derivative of other NSSS thermal power

Fig. 4. The module thermal power responses of multiple MHTGR-based NSSS

directly adjusted in practical engineering, the feasible manipulated variables to compensate $\dot{E}_{i,t}$ are thermal power set-points, which further determines the set-points of nuclear power, temperatures and flowrates. A cascaded structure is then accordingly proposed in Fig. 3, where the NSSS is stabilized in the inner loop by PID and thermal power optimization is achieved in the outer loop.

3. DMC FOR MULTI-MODULAR NSSS

The task of thermal power optimization is to track the thermal command for each NSSS module. Since the accurate model (1) is usually not an easy goal to achieve, in this paper, DMC is considered for thermal power optimization due to the low modelling cost and easy implementation (Moon et al., 2018). To build the step response model, the first derivative step test signal is applied separately to the NSSS control system, and the resultant thermal power responses of all NSSS modules are then sampled and stored at the same time. The modelling steps are described in detail as follows:

Step 1. Set all set-points of NSSS modules to be 75 % reactor full power (RFP), i.e. $Q_{i,0}(0)=0.75\,\mathrm{RFP}$, i=1,2,$\cdots$,m . Then runs simulation software of a multi-MHTGR-based NPPs (Dong et al., 2018).

Step 2. When the thermal power of all modules converges, the derivative of the thermal power set-point of #i NSSS is stepped by α %RFP/Min and the thermal power responses are sampled at every sampling instant denoted as $Q_i(k)$, k is the sampling instant, $k=1,2,\cdots,N$, N is the sampling modelling horizon.

Step 3. The resultant thermal powers are normalized as,

$$s_{ij}(k):=\frac{Q_i(k)-Q_{i,0}(0)}{\alpha\%} \tag{4}$$

where $s_{ij}(k)$ is the normalized data of #i NSSS module excited by #j NSSS module step signal.

Step 4. $s_{ij}(k)$ is then stored in step response coefficient matrix for DMC design,

$$S_{ij}:=\begin{bmatrix} s_{ij}(1) & s_{ij}(2) & \cdots & s_{ij}(N) \end{bmatrix}^{T} \tag{5}$$

The response of thermal powers excited by #1 NSSS module step signal is shown in Fig. 4. When the thermal power set-point derivative signal is stepped by 1 %RFP/min at t = 50000 second, #1 NSSS thermal power is controlled to track the ramp by the inner loop PID control. Other NSSSs show inverse thermal power dynamics due to the feed-water coupling. Derivatives of thermal powers are convergent to a constant value after about 600 seconds. Thus, by selecting to cover the main dynamic transient, the future thermal power can be approximately obtained as,

$$y_i(k+N)=2y_i(k+N-1)-y_i(k+N-2) \tag{6}$$

where y_i is the #i NSSS module thermal power. For state space representation of SRM, define the state variable at k-th instant as,

$$Y_i(k):=\begin{Bmatrix} \left[y_i(k),y_i(k+1),\cdots,y_i(k+N-2),y_i(k+N-1)\right]^{T} \\ \Delta u_i(k+j)=0, \qquad i=0,1,\cdots,\mathrm{m},\ \mathrm{j}=0,1,\cdots \end{Bmatrix}$$

where $\Delta u_i(k) := u_i(k) - u_i(k-1)$, u_i is the derivative signal for #i NSSS module thermal power. Then, the state space model for thermal power optimization can be expressed by,

$$\begin{cases} Y_i(k+1) = MY_i(k) + \sum_{j=1}^{m} S_{ij}\Delta u_j(k) \\ y_i(k) = CY_i(k),\ i = 1,2,\cdots,m \end{cases} \tag{7}$$

where $C = [1\ \ 0\ \ \cdots\ \ 0]_{1\times N}$, and

$$M = \begin{bmatrix} 0 & 1 & 0 & \cdots & 0 & 0 \\ 0 & 0 & 1 & \cdots & 0 & 0 \\ \vdots & \vdots & \vdots & & \vdots & \vdots \\ 0 & 0 & 0 & \cdots & 0 & 1 \\ 0 & 0 & 0 & \cdots & -1 & 2 \end{bmatrix}_{N\times N}$$

From (7), only $y_i(k)$ can be measured, thus a simple linear observer is utilized for state estimation,

$$\begin{aligned} Y_i(k) = MY_i(k-1) + \sum_{j=1}^{m} S_{ij}\Delta u_j(k-1) + \\ K_{f,i}\left(y_i(k-1) - C\hat{Y}_i(k-1)\right) \end{aligned} \tag{8}$$

Based on the model (8) and observer (9), the desirable sequence of derivative revisions is obtained by minimizing a cost function, appropriately defined over prediction horizon as follows:

$$\min_{\Delta u_i(k+j|k)} \sum_{i=1}^{m} J_i(k),\ i = 0,1,\cdots,m, j = 0,1,\cdots,N_c \tag{9a}$$

Subject to the following constraints:

Initial State:

$$Y_i(k|k) = \hat{Y}_i(k) \tag{9b}$$

Prediction Equations:

$$\begin{cases} Y_i(k+l|k) = MY_i(k+l-1|k) + \sum_{j=1}^{m} S_{ij}\Delta u_j(k+l-1|k) \\ y_i(k+l|k) = CY_i(k+l|k),\ l = 1,\cdots,N_p, i = 1,\cdots,m \end{cases} \tag{9c}$$

Constrains on input:

$$\begin{cases} \Delta u_i(k) \in \Xi, i = 1,\cdots,m \\ \Delta u_i(k+j-1|k) = 0,\ j = N_c+1,\cdots,N_p \end{cases} \tag{9d}$$

The objective function takes the following quadratic form:

$$J_i(k) = \sum_{l=1}^{N_p} \left\| r_i(k+l|k) - y_i(k+l|k) \right\|_2^2 + \rho_i \sum_{l=0}^{N_c-1} \left\| \Delta u_i(k+l|k) \right\|_2^2$$

where r_i, ρ_i, N_p and N_c are i-th thermal power command, penalty coefficient, prediction horizon and control horizon, respectively. Ξ is convex set implying the physical limits of thermal power set-points. By solving (9), the set-point trajectories of thermal power for all NSSSs are obtained, but only the first portion of the trajectories, i.e. $\Delta u_i(k)$ is fed to the NSSS control system. At the next sampling time, when the new state estimation $\hat{Y}_i(k+1)$ is ready, the above procedure is repeated.

4. SIMULATION RESULTS

The numerical simulation is performed on MATLAB/ Simulink environment, and the program code is the same as that in Ref. (Dong et al., 2018). The PID controllers in Fig 1c are given as (Dong et al., 2017),

$$\frac{z(s)}{e_n(s)} = \frac{0.5s+0.2}{0.01s+1},\ \frac{\Delta G_{fw}(s)}{e_{Ts}(s)} = 0.5 + \frac{0.02}{s},$$
$$\frac{\Delta G_h(s)}{e_{Ts}(s) - e_{Th}(s)} = 10 + \frac{0.02}{s}$$

where, z, e_n, e_{Ts}, e_{Th}, ΔG_{fw}, ΔG_h are rod speed, set-point deviations of nuclear power, steam and helium temperature, and increments of feedwater and helium flowrate, respectively. The #1-3 NSSS modules and #4-6 NSSS operates at 100% and 50% RFP initially. At 2000s, the thermal powers of 1-3# NSSS manoeuvres from 100% to 75% RFP and from 50% to 75% RFP with a constant velocity of 5%RFP/min, respectively. The responses of key process variables and that of the manipulated variable are shown in Fig. 5-6.

For the case of power manoeuvring, the variation of thermal power set-points leads to the variation of the set-points of nuclear power, temperatures and flowrates of helium and feed-water through communication networks. The control rod, helium blower and feed-water valve, driven by the PID control, immediately adjust the rod speed, helium flowrate and feed-water flowrate to suppress the errors between the measurement and corresponding set-points. The closed-loop stability is well maintained by the inner loop PID control law.

The shortcomings of control scheme in Fig. 2 for thermal power are analysed as follows. Firstly, this control scheme directly use thermal command as the module thermal set-point without further set-point revision to compensate the dynamic of $\dot{E}_{i,t}$, and moreover suppression the error between steam temperature and helium temperature from their set-points is not favourable for heat transfer. Hence based on (2) and (3), a slow convergence of thermal power can be observed after the thermal command stop changing.

The mechanism for the improved thermal power response with DMC is analysed as follows. The DMC explicitly consider the coupling thermal dynamics among NSSS modules in the model (7), and revise the thermal power set-point in the outer loop to compensate the $\dot{E}_{i,t}$ by solving the optimization problem (9). From Fig. 5-6, after the thermal command stop changing, the DMC contributes to a slight overshoot of revised set-point to enhance heat transfer, hence a good thermal command tracking can be observed. From (3), the slow NSSS thermal dynamic is well compensated by the observation of the slow change in thermal power set-point. The thermal coupling among NSSS modules is well suppressed by a small adjustments of thermal power set-point, even if the thermal command remains unchanged.

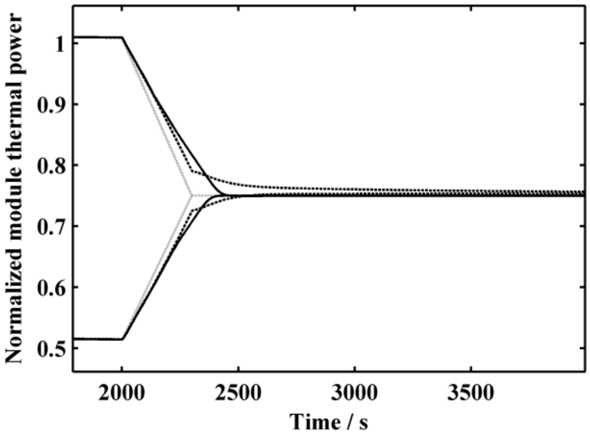

Fig. 5. The normalized module thermal power of multiple MHTGR-based NSSS (solid: DMC; dashed: without DMC; dotted: reference)

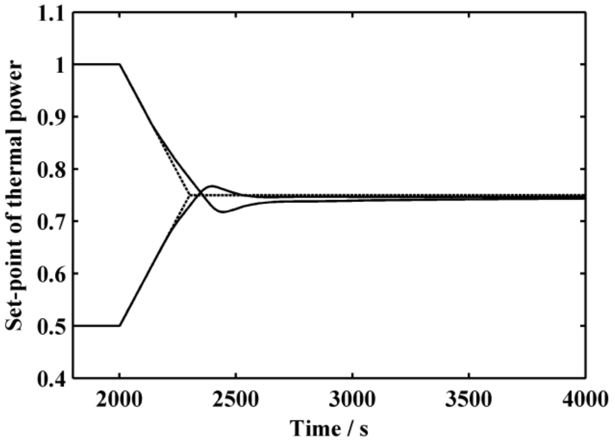

Fig. 6. The set-point of module thermal power of multiple MHTGR-based NSSS

5. CONCLUSIONS

In this paper, a cascade DMC is proposed for thermal power optimization of multi-modular high temperature gas-cooled reactor plants, where inner-loop PID control ensures the closed-loop stability and a multivariable DMC injects revised thermal power set-points in the outer loop. By the dynamic compensation of $\dot{E}_{i,t}$, the proposed method can quickly restore the energy balance among nuclear energy, thermal energy, and load by properly and actively revise the thermal power set-point. This method inherits the existing control system design of the demonstration power station HTR-PM [9-10] and has practical significance for not only improving the load following ability of the multi-module NPPs but also reducing the operator's work intensity.

REFERENCES

Lund, P.D., Lindgren, J., Mikkola, J., and Salpakari, J. (2015). Review of energy system flexibility measures to enable high levels of variable renewable electricity. *Renewable and Sustainable Energy Reviews,* vol. 45, 785–807.

Alizadeh, M.I., Moghaddam, M.P., Amjady, N., Siano, P., and Sheikh-El-Eslami, M.K. (2016). Flexibility in future power systems with high renewable penetration: a review. *Renewable and Sustainable Energy Reviews,* 57, 1186–1193.

Wood, A.J., Wollenberg, B.F., and Sheblé, G.B. (2014). *Power generation, operation and control*, New York: John Wiley & Sons.

Dong, Z., Liu, M., Zhang, Z.Y., Dong, Y.J., and Huang, X.J. (2019). Automatic generation control for the flexible operation of multimodular high temperature gas-cooled reactor plants. *Renewable and Sustainable Energy Reviews,* 108, 11–33.

Locatelli, G., Boarin, S., Pellegrino, F., and Ricotti, M.E. (2015). Load following with small modular reactors (SMRs): a real options analysis. *Renewable and Sustainable Energy Reviews,* 80, 41–54.

Bae, K.H., Kim, H.C., Chang, M.H., and Sim, K.S. (2001). Safety evaluation of the inherent and passive safety features of the smart design. *Annals of Nuclear Energy,* 28(4), 333–349.

Lanning, D.D. (1989). Modularized high-temperature gas-cooled reactor systems. *Nuclear Technology,* 88(2), 139–156.

Garcia, H.E., Chen, J., Kim, J.S., Vilim, R.B., Binder, E.R., Sitton, S.M.B., Boardman, R.D., Mckellar, M.G., and Paredis. C.J.J. (2016). Dynamic performance analysis of two regional nuclear hybrid energy systems. *Energy,* 107, 234–258.

Dong, Z., Pan, Y.F., Zhang, Z.Y., Dong, Y.J., and Huang, X.J. (2018). Dynamical modelling and simulation of the six-modular high temperature gas-cooled reactor plant HTR-PM600. *Energy,* 155(15), 971–991.

Li, G., Wang, X.Q., Liang, B., Li, X., Zhang, B., and Zou, Y. (2016). Modelling and control of nuclear reactor cores for electricity generation: A review of advanced technologies. *Renewable and Sustainable Energy Reviews,* 60, 116–128.

Jiang, D., Dong, Z. (2019). Practical dynamic matrix control of MHTGR-based nuclear steam supply systems. *Energy,* 185(15), 695–707.

Jiang, D., Dong, Z., Liu, M., and Huang, X.J. (2018). Dynamic matrix control for the thermal power of MHTGR-based nuclear steam supply system. *Energies,* 11, 2651.

Moon, U.C., Lee, Y.J., and Lee, K.Y. (2018). Practical dynamic matrix control for thermal power plant coordinated control. *Control Engineering Practice,* 71, 154-163.

Dong, Z., Pan, Y.F., Zhang, Z.Y., Dong, Y.J, and Huang, X.J. (2017). Model-free adaptive control law for nuclear superheated-steam supply systems. *Energy,* 135, 53–67.